Progress in Agricultural Engineering Sciences 19 (2023) 1, 51–68
DOI: 10.1556/446.2023.00071

AKADÉMIAI KIADÓ

Modeling of pressure losses in a cylindrical duct with rectangular ribs

NACER CHOUCHANE[1*], HAMMAM CHOUCHANE[2] and TESNIM CHOUCHANE[3]

[1] Laboratory of Civil Engineering, Hydraulics, Sustainable Development and Environment (LAR-GHYDE), University Mohamed Khider-Biskra, 07000, Algeria

[2] University Mentouri Brothers Constantine, 2500, Algeria

[3] University of Algiers -1- Benyoucef Benkhedda, 1600, Algeria

ORIGINAL RESEARCH PAPER

Received: August 6, 2023 • Accepted: October 9, 2023
Published online: November 20, 2023

ABSTRACT

In order to improve the thermal performance of heat exchangers and air collectors, we insert various forms of artificial roughness, known as ribs, into the useful duct. These ribs promote the creation of turbulent flows and enhance heat transfer by conduction, convection and radiation.

However, the introduction of these ribs leads to an increase in pressure drop, requiring higher mechanical power to pump the heat transfer fluid. This experimental study focuses on estimating, using empirical approaches, the pressure losses induced by rectangular ribs with an inclined top. The ribs are made from 0.4 mm galvanized sheet steel.

An experimental set-up was designed to measure the head losses generated by the ribs, from the point of entry to the point of exit from the useful duct. Using the dimensional analysis method, correlations were established to evaluate head losses as a function of flow regime and rib geometry and configuration (including different geometries for rib arrangement over the configuration area).

KEYWORDS

the head losses, artificial roughness, correlations, ribs, air collectors

* Corresponding author. E-mail: ch_nacer@yahoo.fr

INTRODUCTION

The addition of ribs in the fluid flow stream has an essential objective in optimizing the thermal performance of heat exchangers and particularly in air-mounted solar collectors. To intensify the heat exchange between the exchanges surfaces, various methods are used, among them the addition of metallic obstacles assimilated to artificial roughnesses along the flow plane of the fluid path, which has proved to be of remarkable importance.

Ribs have multiple roles; they contribute to the reduction of dead zones in the liquid stream and enhance the transfer of heat by creating a turbulent flux in the airflow. Their presence translates into significantly higher losses.

Several works were carried out in this field by several authors; we can quote the following works:

Bhagora et al. (2002), Karwa et al. (1999), and Layek et al. (2007, 2009) have treated in their studies the increase of the thermal efficiency of the flux in a rectangular channel provided with transverse ribs, and have also examined the influence of the following geometrical parameters as represented by Fig. 1.

Chaube et al. (2006), Prasad and Saini (1980, 1988, 1991) and Verrma and Prasad (2000) treated only continuous transverse ribs (Fig. 2). They confirmed that the maximum local convective exchange is at the connection points of the flow. They used the coefficient of performance as a parameter for comparison between the different rib configurations and the smooth case.

Instead of using transverse ribs that occupy the entire width of the flow duct (continuous rib), a variant consists of placing discontinuous ribs as shown in Fig. 3 from the study by Cavallero and Tanda (2002). In their studies, they also compared the different configurations shown in Fig. 3 with the smooth case, and the comparison is made here at a fixed and identical flow rate for all the above cases (not at identical pressure losses). The results give, for the continuous transversal ribs, an exchange coefficient of about 2 times compared to the smooth case and of three times for the discontinuous ribs.

Tanda (2004) performed an experimental study on many different rib configurations. For given pressure losses, he found two configurations with equivalent convective transfer levels. These two configurations are shown in Fig. 4a and b.

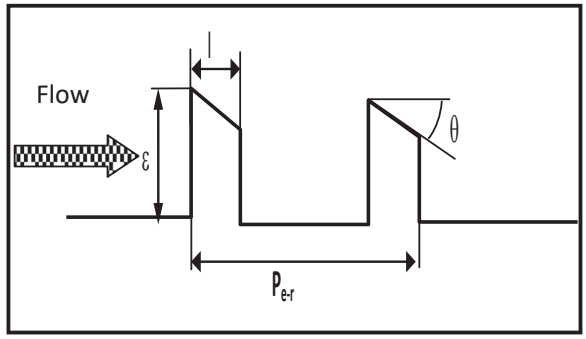

Fig. 1. Geometric parameters of the transverse ribs shaped as ribs

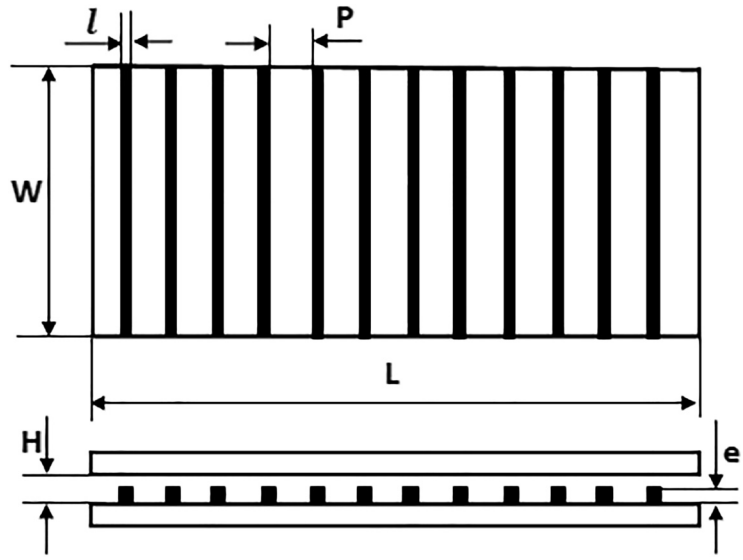

Fig. 2. Continuous rib configurations

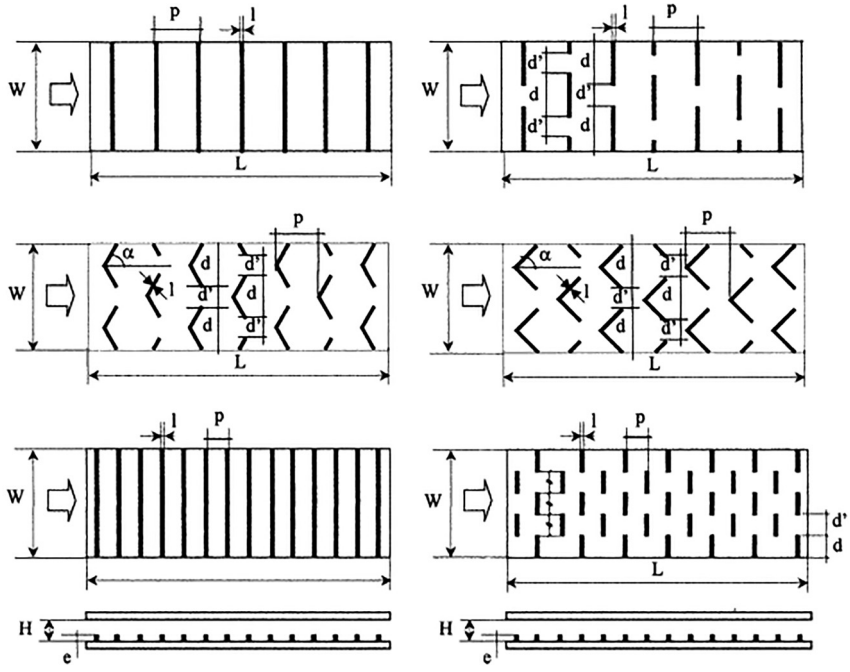

Fig. 3. Continuous and discontinuous rib configurations

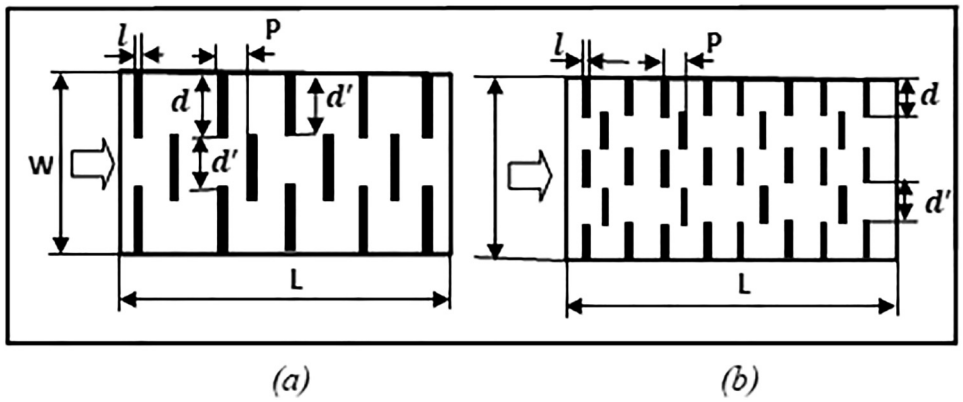

Fig. 4. Discontinuous rib configurations

It is difficult to conclude from the results of Tanda (2004) since he often varied more than one parameter at a time from one configuration to the other; however, it appears that discontinuous ribs offer better thermal performance than continuous ribs.

Tanda (2004), Karwa (2003), Momin et al. (2002), Bhagoria et al. (2002) have performed some works on V-shaped ribs.

The work carried out by Tanda (2004) on V-shaped ribs (Fig. 5), shows that this configuration of ribs is less efficient in comparison with those of continuous transverse shapes, it is however not the result of several authors who also studied similar configurations with this type of fins.

The work of Karwa (2003) and Momin et al. (2002) prove that the best performance is achieved when there is a V-shaped configuration against the flow.

Jaurker et al. (2006) use grooves between two ribs. The results obtained show that in this configuration, the convective exchanges are better than those obtained with ribs in the form of transverse ribs, while the friction coefficient is slightly higher as illustrated in Fig. 6.

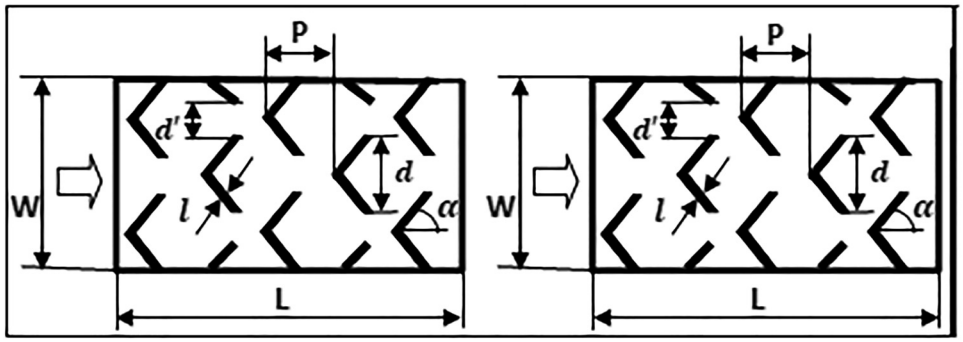

Fig. 5. Duct with ribs arranged in a staggered V-shape

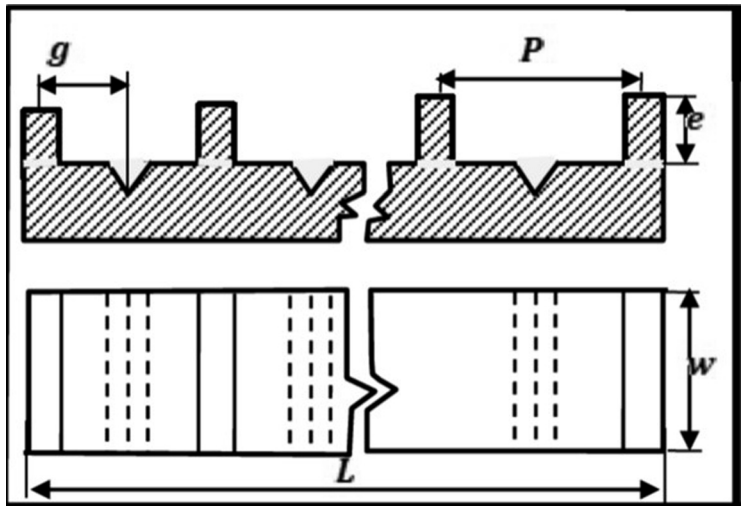

Fig. 6. Configuration with ribs and grooves

In the present work, ribs of rectangular shape are implanted normally to the plane of the flow duct in several rows, with an inclined upper part (Fig. 7). This configuration has multiple reasons:

- Creation of vortices with vertical axes on the flow plane due to sudden narrowing and widening because of reduced spaces between two ribs of the same row.
- The inclined parts of the r form abrupt narrowings and widenings concerning the plane above the flow, which allows the creation of vortices with horizontal axes (Fig. 8) (According to the horizontal axis).
- The combined alternation of vertical and horizontal vortices creates disorder along the flowing moving air stream, which intensifies turbulence and significantly improves convective heat transfer.

EXPERIMENTAL DEVICES

The mechanical engineering department of the University Mohamed khider-Biskra is where the experimental device is produced. It is a cylindrical plastic duct with an overall length of 12 m and a diameter of 160 mm (Fig. 9).

Rectangular aluminum ribs with two parts represent artificial roughness; one part is 1 cm wide with another inclined upper part of 1.5 cm. The incidences of the upper part inclined are 30°, 60°, 120° and 150°.

Inside the duct, the ribs are arranged in two main configurations. One of the configurations is arranged in a uniform row and the other in a random row (Fig. 10a and b). An aspirator provides the airflow and the pressure losses will be measured with a differential pressure sensor. This experimental study consists in measuring the pressure losses between the front and the back of the duct depending on the rate of air volume flow and for various rib arrangements and setups.

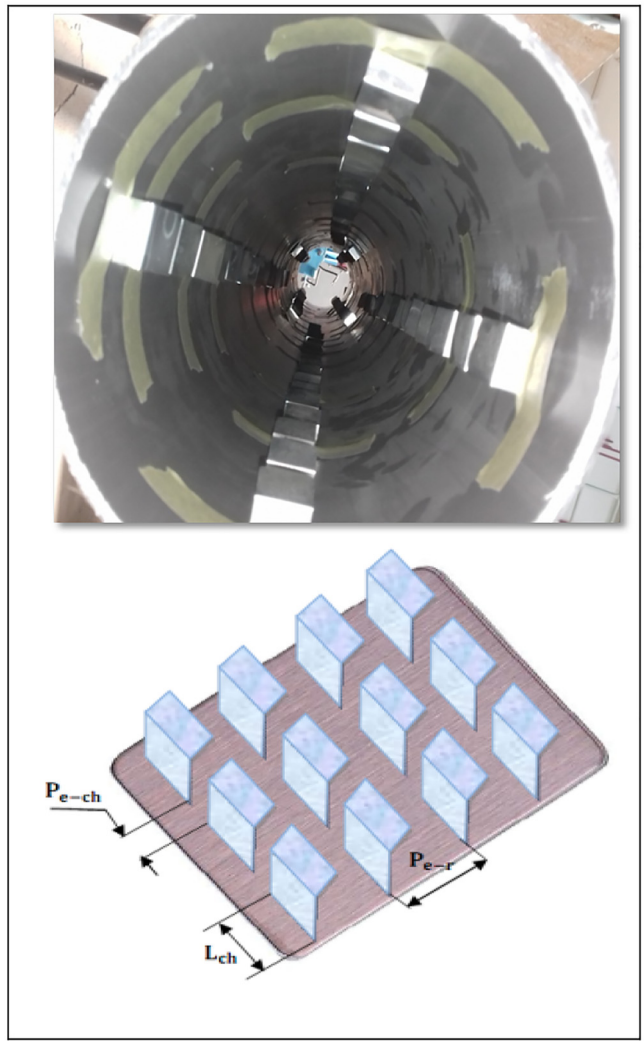

Fig. 7. Rib shapes (rectangular rib)

The measurements of the pressure losses were initially measured for a smooth tube (without ribs) and this is for different values of flow. Secondly, the measurements were made for the various rib configurations (Fig. 10a and b).

OBTAINED RESULTS

The acquired findings demonstrate that, particularly for the 60° and 120° incidences, the pressure losses measured are further amplified in the presence of the ribs. The pressure losses are

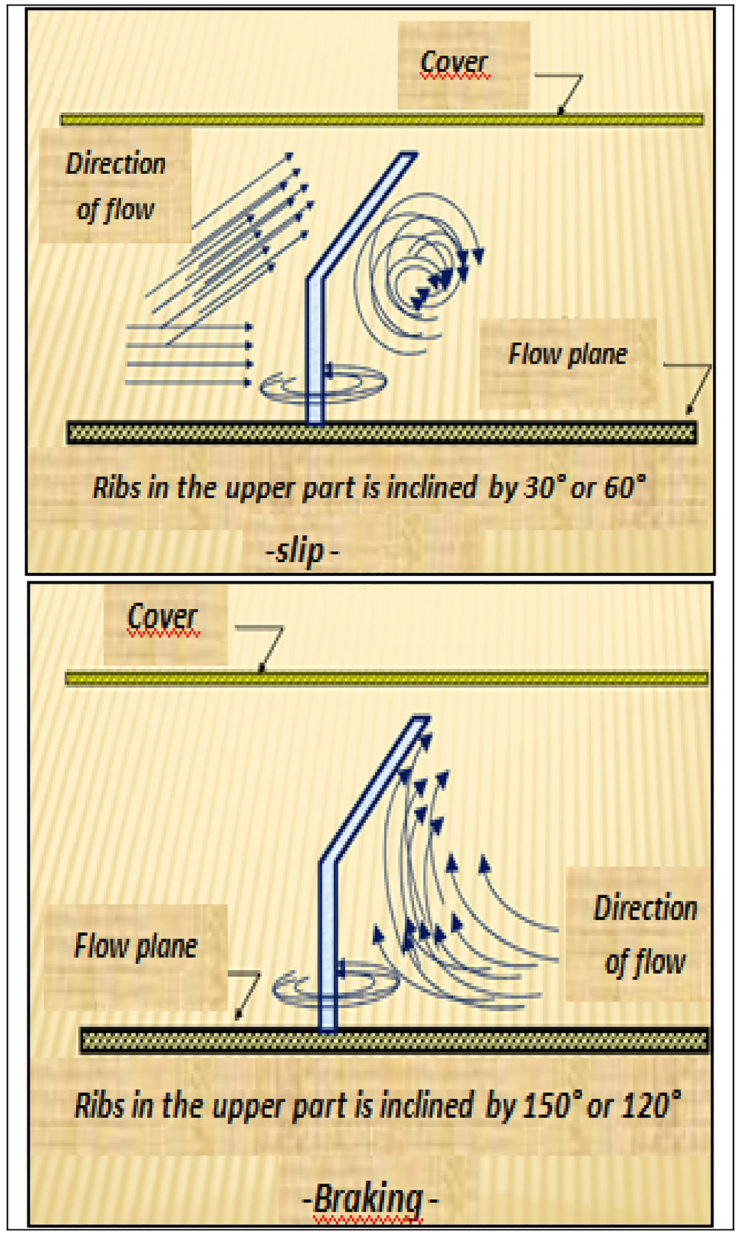

Fig. 8. Scheme of fluid interaction with the ribs

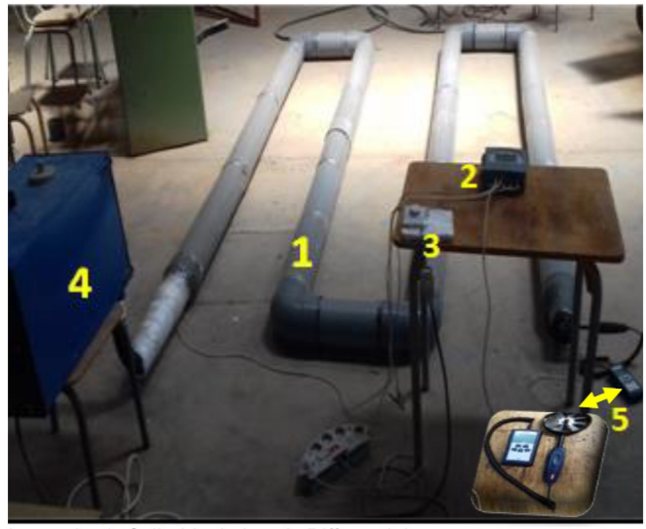

Legends: 1. Cylindrical pipe, 2. Differential manometer,
3. Variable speed drive, 4. Aspirator, 5. Helix anemometer

Fig. 9. Experimental device

more significant in the case of the rib arrangement than when they are aligned in rows when the space between the ribs and the rows is reduced (Figs 11 and 12).

INTERPRETATIONS OF EXPERIMENTAL RESULTS

From the graphs showing pressure drop versus volume flow, we can see that for all configurations generated in the pipe, the pressure drop becomes greater with the presence of ribs than with a smooth pipe (without ribs).

Analysis of pressure drop trends shows that an increase in the pitch between rows or in the pitch between ribs reduces the pressure drop.

As an example, for a common volume flow $Q_v = 0.068 \frac{m^3}{s.m^2}$ and for a rib pitch $P_{e.ch} = 5\ cm$ and a row pitch $P_{e.r} = 6.37\ cm$, the pressure drop reaches a value of 75. 8 *Pascal*, when the pitch between the ribs becomes $P_{e.ch} = 10cm$, and the pitch between the rows $P_{e.r} = 10.5\ cm$, the pressure drop decreases to 62.9 *pascal*.

Contrary to the previous analysis, there is proportionality between the length of the ribs L_{CH} and the rise in pressure drop, where we see that for a common volume flow $Q_v = 0.017 \frac{m^3}{s.m^2}$ and an identical pitch between ribs $P_{e.ch} = 5\ cm$, and for a length of ribs $L_{CH} = 2cm$ the pressure drop is 7.6 *pascal* but as the length increases $L_{ch} = 3cm$ the pressure drop also increases to 8 *pascal*.

Slight deviations from the pressure drop values measured at the various incidences of the upper part of the ribs are noticeable. This is reflected in two phenomena: air slippage in

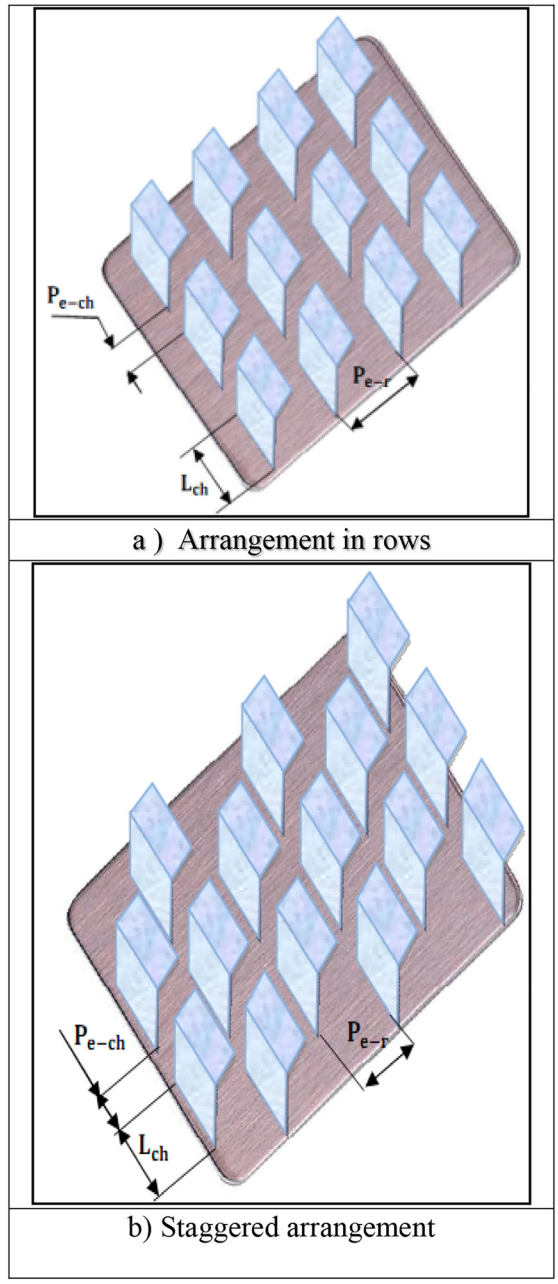

Fig. 10. Rib arrangement scheme

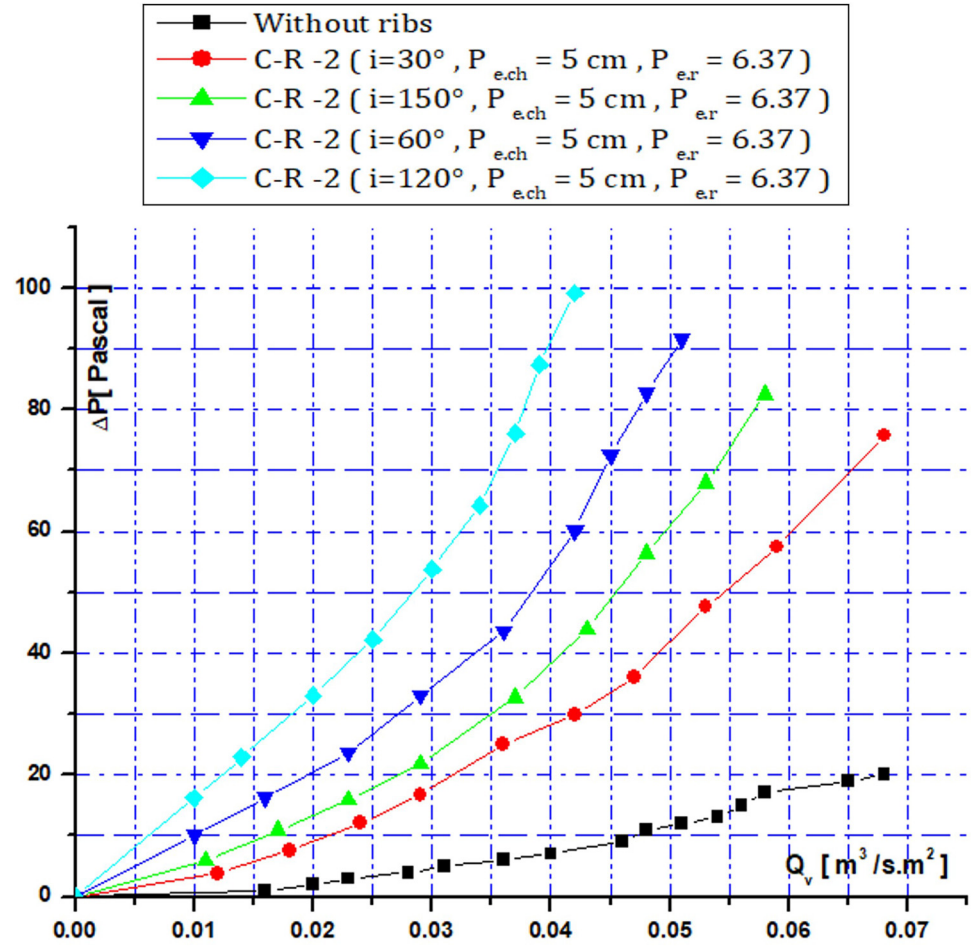

Fig. 11. Evolution of pressure losses depending on the volume flow when there is rectangular ribs arranged in rows versus a smooth duct Case: (L_{ch} = 2cm, $P_{e.ch}$ = 5cm, $P_{e.r}$ = 6.37 cm, i = $30^0, 150^0, 60^0, 120^0$)

relation to the upper part inclined at 30°, 60° and braking at incidences of 150° *and* 120°, see Fig. 8.

ESTABLISHMENT OF THE MATHEMATICAL MODEL OF PRESSURE LOSS CALCULATION

To relate the pressure losses caused by the ribs and their geometrical characteristics as well as the physical parameters of the flowing fluid, we established a general relation based on the fundamental dimensions using the dimensional analysis approach (Vashy-Buckingham theorem), which has the following form:

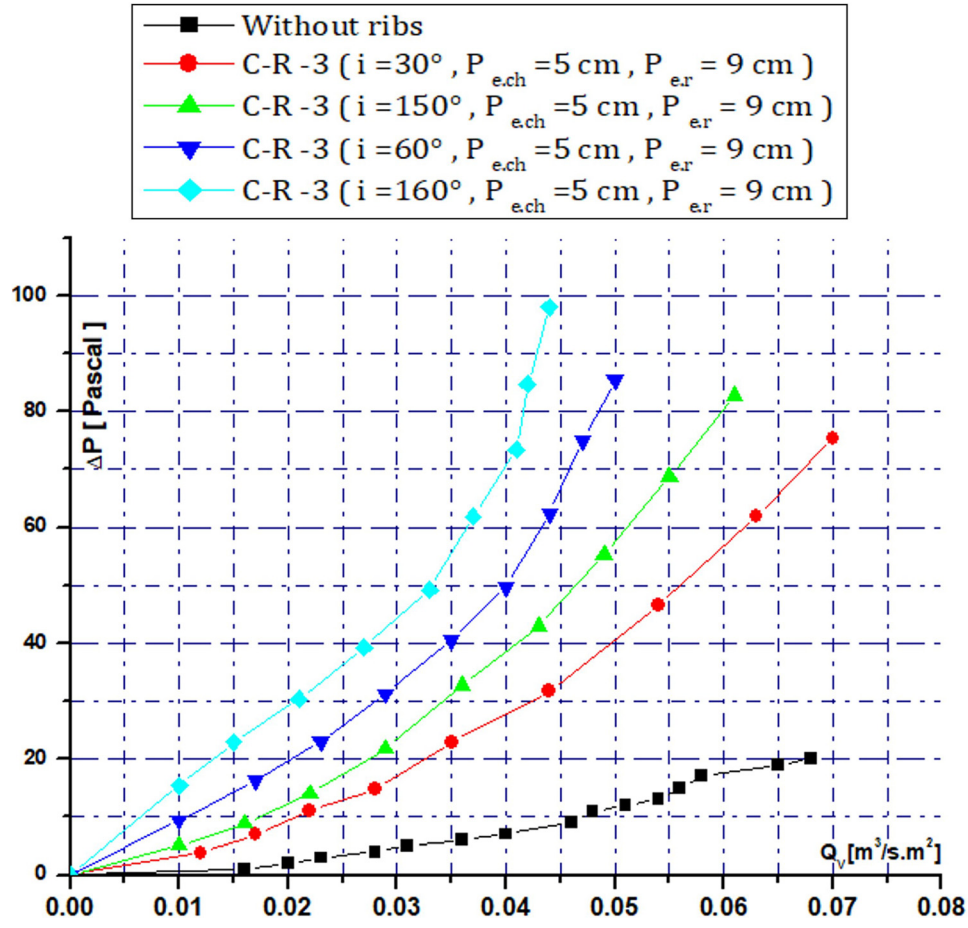

Fig. 12. Evolution of pressure losses depending on the volume flow when there is rectangular ribs in staggered arrangement versus a smooth duct Case:
($L_{ch} = 3cm, P_{e.ch} = 5cm, P_{e.r} = 9.5\ cm, i = 30^0, 150^0, 60^0, 120^0$)

$$\Delta P = \Delta P(\rho, D_H, V, \mu, \varepsilon, L, P_{e.ch}, P_{e.r}, L_{ch}) \tag{1}$$

The π of Vashy-Bukingham theorem states that there are only six possible independent groups. So let us write it as follows, with

L = Constant or L being the length of the cylindrical duct.

$$\left(\frac{\Delta P}{L} = \pi.k.\rho^{\alpha}.D_H^{\beta}.V^{\gamma}.\mu^{x}.\varepsilon^{y}.P_{e.r}^{z}.P_{e.ch}^{t}.L_{ch}^{w}\right) \tag{2}$$

The writing of Eq. (2) taking into account the fundamental dimensions, after development and identification we get a system of three equations, whose solution provides the general expression shown below:

$$\Delta P = \frac{1}{2}\frac{L}{D_H}\rho.V^2.\begin{bmatrix} \left(\frac{\rho v D_H}{\mu}\right)^{-x}.\left(\frac{\varepsilon}{D_H}\right)^{y}\times \\ \left(\frac{P_{e.ch}}{D_H}\right)^{z}.\left(\frac{P_{e.r}}{D_H}\right)^{t}.\left(\left(\frac{L_{ch}}{D_H}\right)\right)^{w} \end{bmatrix} \tag{3}$$

Introducing the Reynolds number, the expression (3) becomes:

$$\Delta P = \frac{1}{2}\frac{L}{D_H}\rho.\begin{bmatrix} (R_e)^{-x}.\left(\frac{\varepsilon}{D_H}\right)^{y}\times \\ \left(\frac{P_{e.ch}}{D_H}\right)^{z}.\left(\frac{P_{e.r}}{D_H}\right)^{t}.\left(\left(\frac{L_{ch}}{D_H}\right)\right)^{w} \end{bmatrix}.V^2 \tag{3'}$$

The identification with respect to the general equation of the pressure losses allows us to obtain a coefficient of the pressure losses λ given by the expression:

$$\lambda = \begin{bmatrix} (R_e)^{-x}.\left(\frac{\varepsilon}{D_H}\right)^{y}\times \\ \left(\frac{P_{e.ch}}{D_H}\right)^{z}.\left(\frac{P_{e.r}}{D_H}\right)^{t}.\left(\left(\frac{L_{ch}}{D_H}\right)\right)^{w} \end{bmatrix} \tag{4}$$

A simple development of Eq. (3)' gives us:

$$ln\left(\frac{2\Delta P D_H}{L\rho V^2}\right) = -xln((R_e)) + yln\left(\left(\frac{\varepsilon}{D_H}\right)\right) + zln\left(\left(\frac{P_{e.ch}}{D_H}\right)\right) + tln\left(\left(\frac{P_{e.r}}{D_H}\right)\right) + wln\left(\frac{L_{ch}}{D_H}\right) \tag{5}$$

Ribs arranged in rows

In the case of a turbulent regime, the identification of the geometric parameters of the ribs with respect to the relation (5) which gives in its developed form ΔP, allows to obtain several systems of equations.

We derive the system of equations by using the relation (5):

$$\left[A_{i,j}\right].X = [B] \Big/ \begin{bmatrix} i = 1, \ldots\ldots, n \\ j = 1, \ldots\ldots, 5 \\ n = 100 \end{bmatrix}$$

We notice that the matrix $\boldsymbol{A_{i,j}}$ is not square.

The least squares approach is used to solve this system:

$$A_{i,j}{}^{T}.A_{i,j}X = A_{i,j}{}^{T}.[B] \Big/ \begin{bmatrix} i = 1, \ldots., n \\ j = 1, \ldots\ldots, 5 \\ n = 100 \\ \left[A_{i,j}\right]^{T} : \text{Matrix transpose of } A_{i,j} \end{bmatrix}$$

We obtain a system of equations:

$$\left[A_{i,j}{}^{T}.A_{i,j}\right]X = A_{i,j}{}^{T}.B = C_{k,m}X = D_{l,f} \Big/ \begin{bmatrix} k = 1, \ldots., 5 \\ m = 1, \ldots\ldots, 5 \\ l = 1, \ldots\ldots, 5 \\ f = 1 \end{bmatrix}$$

By the Gaussian elimination, we find the solutions.

We replace the solutions in Eq. (3)' and obtain the following correlation:

$$\Delta P = \frac{1}{2}\frac{L}{D_H}\rho \begin{bmatrix} (R_e)^{-0.9414}.\left(\dfrac{\varepsilon}{D_H}\right)^{3.992} \\ \times\left(\dfrac{P_{e.ch}}{D_H}\right)^{-3.9334} \\ \times\left(\dfrac{P_{e.r}}{D_H}\right)^{5.8817}.\left(\dfrac{L_{ch}}{D_H}\right)^{-4.9624} \end{bmatrix}.V^2$$

And therefore the pressure loss coefficient is:

$$\lambda = \begin{bmatrix} (R_e)^{-0.9414}.\left(\dfrac{\varepsilon}{D_H}\right)^{3.992} \\ \times\left(\dfrac{P_{e.ch}}{D_H}\right)^{-3.9334} \\ \times\left(\dfrac{P_{e.r}}{D_H}\right)^{5.8817}.\left(\dfrac{L_{ch}}{D_H}\right)^{-4.9624} \end{bmatrix}$$

The same procedure of calculation is followed for the other studied cases, which means that in the interval of the turbulent regime one arrives at practically the same expression of the pressure losses.

For a laminar flow regime $Re \leq 2100$, the expression of the pressure losses is as follows:

$$\Delta P = \frac{1}{2}\frac{L}{D_H}\rho \begin{bmatrix} (R_e)^{-1.2031}.\left(\dfrac{\varepsilon}{D_H}\right)^{-0.2627} \\ \times\left(\dfrac{P_{e.ch}}{D_H}\right)^{0.6427} \\ \times\left(\dfrac{P_{e.r}}{D_H}\right)^{0.7942}.\left(\dfrac{L_{ch}}{D_H}\right)^{0.8135} \end{bmatrix}.V^2$$

Whose pressure loss coefficient is:

$$\lambda = \begin{bmatrix} (R_e)^{-1.2031} \cdot \left(\frac{\varepsilon}{D_H}\right)^{-0.2627} \\ \times \left(\frac{P_{e.ch}}{D_H}\right)^{0.6427} \\ \times \left(\frac{P_{e.r}}{D_H}\right)^{0.7942} \cdot \left(\frac{L_{ch}}{D_H}\right)^{0.8135} \end{bmatrix}$$

Ribs arranged in staggered rows

The same experimental approach is also performed with this arrangement, which allowed us to obtain the following correlations.

- For a turbulent flow regime:

$$\Delta P = \frac{1}{2}\frac{L}{D_H}\rho \begin{bmatrix} (R_e)^{-0.9046} \cdot \left(\left(\frac{\varepsilon}{D_H}\right)^{4.381} \right. \\ \times \left(\frac{P_{e.ch}}{D_H}\right)^{-4.1435} \\ \times \left(\frac{P_{e.r}}{D_H}\right)^{5.8853} \cdot \left(\frac{L_{ch}}{D_H}\right)^{-5.1682} \end{bmatrix} . V^2$$

And consequently a pressure loss coefficient λ:

$$\lambda = \begin{bmatrix} (R_e)^{-0.9046} \cdot \left(\left(\frac{\varepsilon}{D_H}\right)^{4.381} \right. \\ \times \left(\frac{P_{e.ch}}{D_H}\right)^{-4.1435} \\ \times \left(\frac{P_{e.r}}{D_H}\right)^{5.8853} \cdot \left(\frac{L_{ch}}{D_H}\right)^{-5.1682} \end{bmatrix}$$

- For the laminar flow regime:

$$\Delta P = \frac{1}{2}\frac{L}{D_H}\rho \begin{bmatrix} (R_e)^{-1.2675} \cdot \left(\frac{\varepsilon}{D_H}\right)^{0.3243} \\ \times \left(\frac{P_{e.ch}}{D_H}\right)^{0.2084} \\ \times \left(\frac{P_{e.r}}{D_H}\right)^{1.5326} \cdot \left(\frac{L_{ch}}{D_H}\right)^{-0.096} \end{bmatrix} . V^2$$

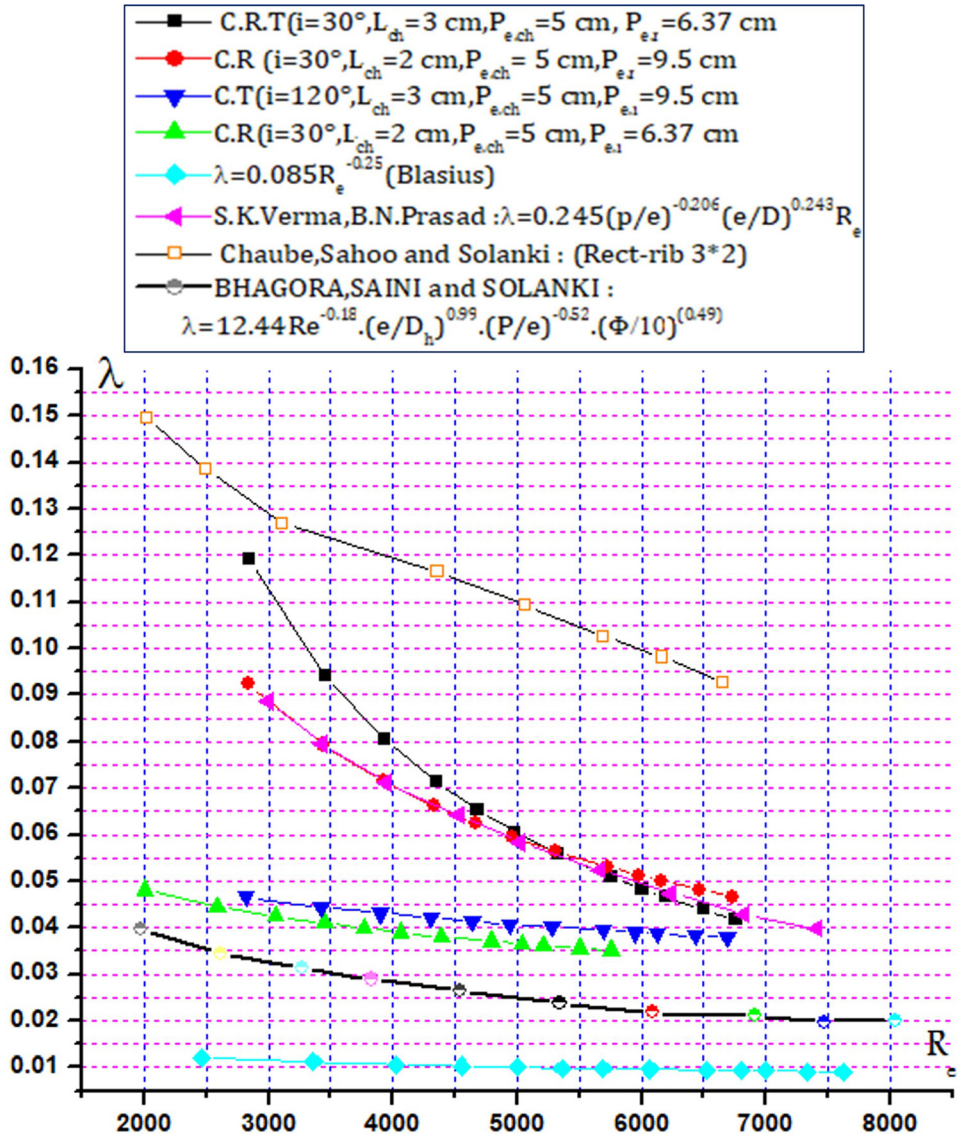

Fig. 13. Pressure loss coefficient λ depending on Reynolds, compared with the Blasius, S.K. Verma, Chaube and Bhagora models (Row ribs)

For which the pressure loss coefficient is:

$$\lambda = \left[\begin{array}{c} (R_e)^{-1.2675} \cdot \left(\frac{\varepsilon}{D_H}\right)^{0.3243} \\ \times \left(\frac{P_{e.ch}}{D_H}\right)^{0.2084} \\ \times \left(\frac{P_{e.r}}{D_H}\right)^{1.5326} \cdot \left(\frac{L_{ch}}{D_H}\right)^{-0.096} \end{array} \right]$$

Evolution of the pressure losses coefficient λ depending on Reynolds

From the developed correlations, which express the pressure loss coefficient based on the ribs' taken-in geometrical characteristics, on the geometry of disposition and on the flow regime, it was possible to elaborate graphs which show the evolution of λ depending on the Reynolds number, for the different configurations of the ribs studied in relation to a smooth duct, on the other hand, in order to verify the accuracy of the numerical process adjustment followed in this work, and the good agreement of the empirical models developed with others encountered in the literature, in particular with those of Blasius & all, S. K. Verma & all, Chaube & all and Bhagoria & all, whose analysis of the evolution of the pressure loss coefficients illustrated in Fig. 13 shows the agreement of the empirical models related to the configurations of the ribs studied.

CONCLUSION

The correlations obtained make it possible to estimate the pressure losses in a rectangular duct, whose flow plane is occupied by obstacles of various shapes and arrangements. The recorded measurements of the pressure drop show that they are more important with the staggered arrangement of the ribs, especially for the strong incidences of the inclined part of them.

The empirical equations established will constitute technical support for future studies, which are essential to enhance heat exchangers' thermal efficiency and particularly of flat air-mounted solar collectors.

For other shapes, the general equation is still applicable, which will be the subject of further comprehensive studies, whose main interest is to be able to imagine the optimal shapes that will contribute to improving the heat exchange and in this case, will give a compromise between the pressure losses generated and the output temperature obtained.

ACKNOWLEDGEMENTS

Not applicable.

NOMENCLATURE

ΔP	Pressure losses $[Pascal]$
ρ	Density of the air $[kg/m^3]$
D_H	Hydraulic diameter $[m]$
V	air velocity $[m/s]$
μ	Dynamic viscosity $[Kg/m.s]$
ε	Absolute roughness $[m]$
L	Duct length $[m]$
$P_{e.ch}$	Steps between the ribs $[m]$
$P_{e.r}$	Steps between two successive rows of ribs $[m]$
L_{ch}	Length of a rib $[m]$
C-R-2	Rectangular rib 2 [cm] long
C-R-3	Rectangular rib 3 [cm] long

REFERENCES

Bhagoria, J.L., Saini, J.S., and Solanki, S.C. (2002). Heat transfer coefficient and friction factor correlations for rectangular solar air heater duct having transverse wedge shaped rib roughness on the absorber plate. *Renewable Energy*, 25: 341–369. https://doi.org/10.1016/S0960-1481(01)00057-X.

Cavallero, D. and Tanda, G. (2002). An experimental investigation of forced convection heat transfer in channels with rib turbulators by means of liquid crystal thermography. *Experimental Thermal and Fluid Science*, 26(2–4): 115–121. https://doi.org/10.1016/S0894-1777(02)00117-6.

Chaube, A., Sahoo, P.K., and Solanki, S.C. (2006). Analysis of heat transfer augmentation and flow characteristics due to rib roughness over obserber plate of a solar air heater. *Renewable Energy*, (3): 317–331. https://doi.org/10.1016/j.renene.2005.01.012.

Jauker, A.R., Saini, J.S., and Gandhi, B.K. (2006). Heat transfer and friction characteristics of rectangular solar air heater duct using – grooved artificial roughness. *Solar Energy*, 80(8): 895–907. https://doi.org/10.1016/j.solener.2005.08.006.

Karwa, R. (2003). Experimental studies of augmented heat transfer and friction in asymmetrically heated rectangular ducts with ribs on the heated wall in transverse, inclined, v-continuous and v-discrete pattern. *Heat and Mass Transfer*, 30(2): 241–250. https://doi.org/10.1016/S0735-1933(03)00035-6.

Karwa, R., Solanki, S.C., and Saini, J.S. (1999). Heat transfer coefficient and friction factor correlations for the transient flow regime in rib–roughened rectangular ducts. *International Journal of Heat and Mass Transfer*, 42(9): 1597–1615. https://doi.org/10.1016/S0017-9310(98)00252-X.

Layek, A., Saini, J.S., and Solanki, S.C. (2007). Heat transfer and friction characteristics for artificially roughened ducts with compound turbulators. *International Journal of Heat and Mass Transfer*, 50: 4845–4854. https://doi.org/10.1016/j.ijheatmasstransfer.2007.02.042.

Layek, A., Saini, J.S., and Solanki, S.C. (2009). Effect of chamfering on heat transfer and friction characteristics of solar air heated having absorber plate roughened with compound turbulators. *Renewable Energy*, 34: 1292–1298. https://doi.org/10.1016/j.renene.2008.09.016.

Momin, A.M.E., Saini, J.S., and Solanki, S.C. (2002). Heat transfer and friction in solar air heater duct with Vshaped rib roughness on absorber plate. *International Journal of Heat and Mass Transfer*, 45(16): 3383–3396, July. https://doi.org/10.1016/S0017-9310(02)00046-7.

Prasad, B.N. and Saini, J.S. (1980). Effect of artificial roughness on heat transfer and friction factor in solar air-heaters. *Solar Energy*, 41(6): 505–560. https://doi.org/10.1016/0038-092X(88)90058-8.

Prasad, B.N. and Saini, J.S. (1988). Effect of artificial roughness on heat transfer and friction factor in a solar air heater. *Solar Energy*, 41: 555–560. https://doi.org/10.1016/0038-092X(88)90058-8.

Prasad, B.N. and Saini, J.S. (1991). Optimal thermohydrolic performance of artificially roughened solar air heating. *Solar Energy*, 47(2): 91–96. https://doi.org/10.1016/0038-092X(91)90039-Y.

Tanda, G. (2004). Heat transfer in rectangular channels with transverse and V-shaped broken ribs. *International Journal of Heat and Mass Transfer*, 47: 229–243. https://doi.org/10.1016/S0017-9310(03)00414-9.

Verrma, S.K. and Prasad, B.N. (2000). Investigation for the optimal thermo hydraulic performance of artificially roughened solar air heaters. *Renewable Energy*, 20: 19–36. https://doi.org/10.1016/S0960-1481(99)00081-6.